

A Hybrid Emulsion Detector

For

Direct Observation of ν_τ

The DONUT Collaboration

K. Kodama^a, N. Ushida^a, S. Aoki^b, T. Hara^b, N. Hashizume^c, K. Hoshino^c, H. Iinuma^c, K. Ito^c, M. Kobayashi^c, M. Miyanashi^c, M. Komatsu^c, M. Nakamura^c, K. Nakajima^c, T. Nakano^c, K. Niwa^c, N. Nonaka^c, K. Okada^c, T. Yamamori^c, H. Okabe^d, M. Adachi^e, M. Kazuno^e, Y. Kobayashi^e, E. Niu^e, S. Ono^e, H. Shibuya^e, Y. Umezawa^e, Y. Sato^f, I. Tezuka^f, P. Yager^g, B. Baller^h, D. Boehnlein^h, W. Freeman^h, B. Lundberg^{h*}, J. Morfin^h, R. Rameika^h, P. Berghausⁱ, M. Kubansteⁱ, N. W. Reayⁱ, R. Sidwellⁱ, N. Stantonⁱ, S. Yoshidaⁱ, D. Ciampa^j, C. Erickson^j, K. Heller^j, R. Rusack^j, R. Schwienhorst^j, J. Sielaff^j, J. Trammell^j, J. Wilcox^j, T. Akdogan^k, V. Paolone^{k*}, F. Avignone^l, A. Kulik^l, C. Rosenfeld^l, A. Napier^m, T. Kafka^m, W. Oliver^m, J. Schneps^m, M. Skender^m, T. Patzak^m, C. Andreopoulosⁿ, G. Tzanakosⁿ, N. Saolidouⁿ, J. S. Song^p, I. G. Park^p, S. H. Chung^p, C. H. Hahn^q, J. Y. Kim^r, J. T. Rhee^s, S. N. Kim^t, W. H. Chung^u, S. Y. Bahk^v

^a Aichi University of Education, ^b Kobe University, ^c Nagoya University, ^d Science Education Institute of Osaka Prefecture, ^e Toho University, ^f Utsunomiya University, ^g University of California at Davis, ^h Fermilab, ⁱ Kansas State University, ^j University of Minnesota, ^k University of Pittsburgh, ^l University of South Carolina, ^m Tufts University, ⁿ University of Athens, ^p Gyeongsang National University, ^q Changwon National University, ^r Chonnam National University, ^s Kon-Kuk University, ^t Korean National University of Education, ^u Pusan National University, ^v Wonkwang University

* Spokespersons

Abstract

An experimental apparatus, designed primarily for direct observation of the tau neutrino, has been constructed and made operational by the DONUT Collaboration for the Fermilab E872 experiment. It consists of a nuclear emulsion target, a scintillating fiber tracker system with optoelectronic readout, an air-core analysis magnet, trigger counters, drift chambers, an electromagnetic calorimeter, and a muon identification system. The design, construction and performance of the entire apparatus and of the various detectors are described.

1 Introduction

The E872 experiment was proposed to directly observe the charged current interaction of the tau neutrino, [1]. There is compelling theoretical justification and experimental evidence that the tau neutrino (ν_τ) exists as a unique lepton [2, 3]. Experimental evidence to date indicates that the couplings of the ν_τ are consistent with predictions of the Standard Model [4, 5]. However, direct interactions of ν_τ in the manner observed for ν_e and ν_μ have yet to be seen. Experimental observation of charged-current ν_τ events requires high beam intensity combined with very good detector resolution. These requirements are met by the 800 GeV primary proton beam from the Fermilab Tevatron combined with a hybrid emulsion spectrometer. The hybrid emulsion spectrometer consists of a nuclear emulsion target and ancillary detectors for event location. This same technique has been used successfully in other experiments [6, 7, 8].

Recent experimental data [9] indicate that the atmospheric neutrino anomaly might be due to neutrino flavor oscillations of the type $\nu_\mu \rightarrow \nu_\tau$. In addition to the experiments of references 6 and 8, other oscillation experiments,

both short-baseline and long-baseline, have considered the use of high resolution emulsion targets to detect neutrino oscillations through the direct observation of μ from a beam initially composed of μ [10, 11, 12]. The E872 experiment is, therefore, an important step in the methodology of addressing questions of neutrino mass and mixing.

The E872 experiment tested the detector components early in the Tevatron 1996-97 fixed target run and collected physics data from 13 April, 1997, when the first two emulsion modules were installed, to 3 September, 1997. Altogether, a total of seven emulsion modules were used, although no more than four were used at any given time.

We describe the experimental apparatus in this paper, with particular emphasis on the design, construction and performance of the various detector subsystems. The prompt neutrino beam is presented in a separate paper.

2 Conceptual Design

Tau neutrinos are produced predominantly from the leptonic decay of the D_S meson in the decay sequence

$$D_S \rightarrow \tau + \nu_\tau \quad \bar{\nu}_\tau + X \quad 1.$$

In this experiment D_S mesons are produced by 800 GeV protons interacting in a tungsten beam dump. Both the D_S and the daughter τ decay in the dump, each decay producing one ν_τ (neutrino or antineutrino). The number of ν_τ per incident proton produced in the beam dump through this process is estimated to be 1.68×10^{-4} [13].

Observation of a τ interaction is made by observing the τ lepton, produced in the charged current interaction $\nu + N \rightarrow \tau + X$, and the subsequent decay of the τ in an active target. The τ lepton has a c of 0.087 mm and therefore will decay within a distance of ~ 5 mm ($\langle c \rangle = 2.5$ mm for a 50 GeV/c τ). Eighty-six per cent of the τ decays have only one charged track (a “kink” decay). This implies that a very high spatial resolution on tracks near the vertex is required. Nuclear emulsion was chosen as the neutrino interaction target since it provides the very high resolution necessary to resolve τ decays, as well as sufficient mass to produce a reasonable event rate. The τ interaction candidates are recognized by the topology of the tracks associated with the neutrino interaction vertex. The primary characteristics of the decay, which can be measured with an emulsion target, are the direction of the tau with respect to the incoming neutrino, the decay length of the tau, the angle(s) between the tau and its daughter(s), and the momentum of the daughter(s).

The number of τ charged-current interactions that occur per centimeter of target material is determined by the τ energy and interaction cross section. Because the τ interaction cross section depends on the energy of the τ , the neutrinos from each of the decays ($D_S \rightarrow \tau + \nu$ and $\nu + X$) have different interaction probabilities. For the purposes of estimating expected event rates we have used an effective interaction cross section of $0.42 \times 10^{-37} \text{ cm}^2$ [14]. The solid angle acceptance of the E872 target was ± 7.1 mr, within which we calculate 5.0×10^{-18} charged-current interactions per centimeter of emulsion ($\rho = 3.72 \text{ g/cm}^3$) per proton. Taking into account τ sources other than D_S , such as B

increases the predicted yield by 14% to 5.8×10^{-18} charged-current interactions per centimeter of emulsion per proton.

The target configuration described in Section 4 was chosen to optimize the number of interactions while retaining the ability to find and measure the events with high efficiency. An added constraint was the high cost of the nuclear emulsion, ~\$300K per 100 kg.

While an emulsion target is “active” in the sense that it records the tracks produced at the interaction vertex, it is passive in the sense that it has no electronic output indicating when an interaction has occurred. It simply records all tracks that are produced in it or pass through it. In order to untangle interesting interactions from the background, an electronic spectrometer is used to trigger a data acquisition system, which records the signals from the particles that emerge from the emulsion targets. The electronic spectrometer, in conjunction with the emulsion target is called a hybrid emulsion spectrometer (HES). As a consequence of cost and schedule constraints, many of the components used in the E872 HES were recycled from previous Fermilab experiments. A plan view of the E872 HES is shown in Figure [].

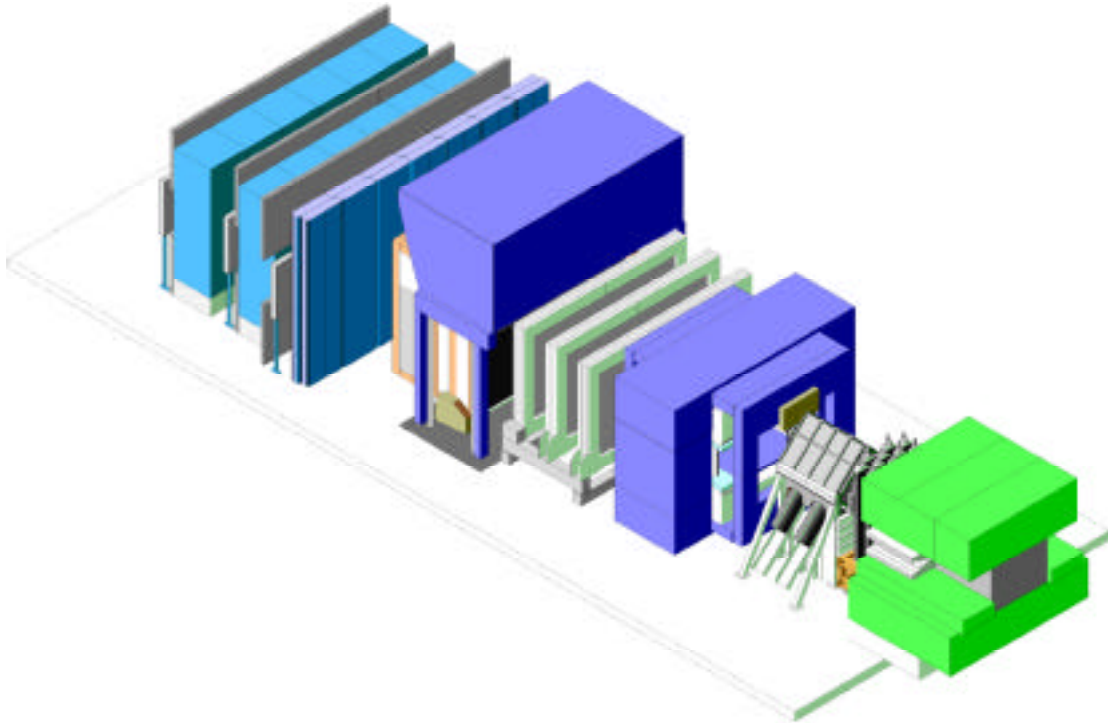


Figure 1. The DONUT hybrid emulsion spectrometer. The beam direction is from the lower left to the upper right. The components, proceeding downstream, include shielding, veto counter, target box containing emulsion modules and scintillating fiber trackers, analysis magnet, drift chambers, electromagnetic calorimeter and muon identification system.

The major task of the electronic spectrometer is to reconstruct tracks from the neutrino interaction vertex. The location of the primary interaction in the emulsion requires, at a minimum, a single non-interacting reconstructed spectrometer track projected to a vertex candidate in the emulsion, where an emulsion vertex is defined as one or more tracks *originating* in the emulsion target. The configuration of the electronic spectrometer is meant to provide a series of particle tracking devices that optimize acceptance and position resolution. To do this detectors with large acceptance but poor resolution are placed at the downstream end of the spectrometer. Smaller, but high resolution tracking is placed in the upstream section, allowing for precision tracking into

the emulsion modules. In addition to the emulsion target modules the major components of the HES are:

- Emulsion sheets that are frequently replaced to keep the track density very low for event identification. These “changeable sheets” (at 8 locations) were replaced about once every week;
- A 60,000 channel scintillating fiber detector arranged in 44 tracking planes. It has sufficient resolution to point tracks from the wire chambers to special emulsion sheets;
- Three planes of scintillation counters to provide signals for a trigger;
- A large aperture dipole magnet to provide a 225 MeV/c p_T kick for momentum analysis (ROSIE);
- Drift chamber tracking upstream and downstream of the analysis magnet;
- An electromagnetic calorimeter to aid in the identification of electrons and contribute to the measurement of the total energy in the event;
- A muon tagging system using range to screen out hadrons and provide identification of muons.

Subsequent sections of this paper will describe the configuration and performance of each system in detail.

3 The Prompt Neutrino Beam

Protons accelerated to 800 GeV/c in the Fermilab Tevatron were directed onto a tungsten target to produce a prompt neutrino beam. Such a beam is characterized by an enhanced proportion of neutrinos from the decay of short-lived particles. Most pions and kaons, which ordinarily are the valued particles in neutrino beam design, interact before they have a chance to decay. The target is 10 cm × 10 cm in cross section and 100 cm (10.4 nuclear interaction lengths)

long. Only about 0.1% of the pions produced in this target decay to produce neutrinos.

The important particles in the beam dump interaction are the charmed particles, which have a typical lifetime of about 10^{-12} s. These can decay leptonically before they interact in the target, producing e , e , μ , μ , ν , and $\bar{\nu}$. The electrons are absorbed by the dump, the muons penetrate the dump, and the leptons decay to produce an additional neutrino. The three flavors of neutrinos make up the prompt neutrino beam.

The muons produced in the tungsten beam dump were the most challenging component of background exposure to the emulsion. The muon exposure was controlled by both active and passive means. A set of sweeping magnets (SELMA and MUSWEEP2), placed immediately downstream of the dump, diverted low-momentum muons away from the emulsion target 36 m downstream. Beyond the sweeping magnets, steel shielding, partially shown in Figure 1, ranged out most of the muons that passed through the magnets. The goal was to keep the muon tracks in the emulsion to fewer than 10^5 per cm^2 . The passive shielding was optimized with calculations by N. V. Mokhov using the MARS Monte Carlo code [15]. The optimization mainly involved removing steel shielding from the regions of the muon plumes created by the sweeping magnets. Muon interactions in the steel can produce considerable electromagnetic showers in the target area. Most of the shielding volume from which steel was removed was left empty, although some was replaced with polyethelene as shielding from electromagnetic showers. The optimized shielding reduced background radiation levels by a factor of 50 to 100.

The neutrino flux that was the result of the prompt neutrino beam system was calculated to consist of ν_μ (52%), ν_e (44%) and ν_τ (5%) (with equal numbers of ν and $\bar{\nu}$). On average, three neutrino interactions were recorded per hour at the emulsion targets under normal operating conditions (5×10^{14} 800 GeV protons per hour). A total of 4.5×10^{17} protons were used during the entire experiment. The neutrino spectrum has been measured to have a mean energy of 82 ± 5 GeV for the ν_μ component, in agreement with design expectations. The prompt neutrino beam designed and built for DONUT is described in further detail by Schwienhorst [16].

4 The Emulsion Target

The heart of the DONUT experiment is the target box, which contains four separate modules aligned and mounted on a precision stand. Each module is made from emulsion sheets, 50 cm \times 50 cm in area, oriented perpendicular to the beam. A module contains from 50 to 80 individual sheets, depending on the module design, compressed tightly together under vacuum to form a solid unit 6 cm thick. The thickness of the emulsion coating on the sheets varied, depending on the type and location of the module, as discussed below.

In order to minimize the total volume of emulsion to be scanned, the exit points of tracks leaving the modules must be precisely located. To achieve this precision, the target modules are separated by layers of scintillating fibers and special emulsion sheets separate from the modules. These special emulsion sheets are useful only if their track density is much lower than that of the sheets within the module; ideally they should contain of order 1 track per field of view when scanned. The low track density is achieved by replacing the special sheets,

known as "changeable sheets", approximately once per week. Thus, the location of tracks within a module follows a chain of increasing precision: Detectors of moderate resolution (drift chambers) are used to find tracks in detectors of higher resolution (scintillating fibers), which, in turn, are used to extrapolate tracks into the changeable sheets. Tracks found in the changeable sheets allow a precise extrapolation into the target module itself.

A diagram depicting the target box configuration is shown in Figure 2. The exterior of the box was covered with a layer of lead, varying from 13 mm to 20 mm in thickness, to protect the emulsion from the ambient radiation during the experimental run.

The type of emulsion used is Fuji EHT 007/008 48.

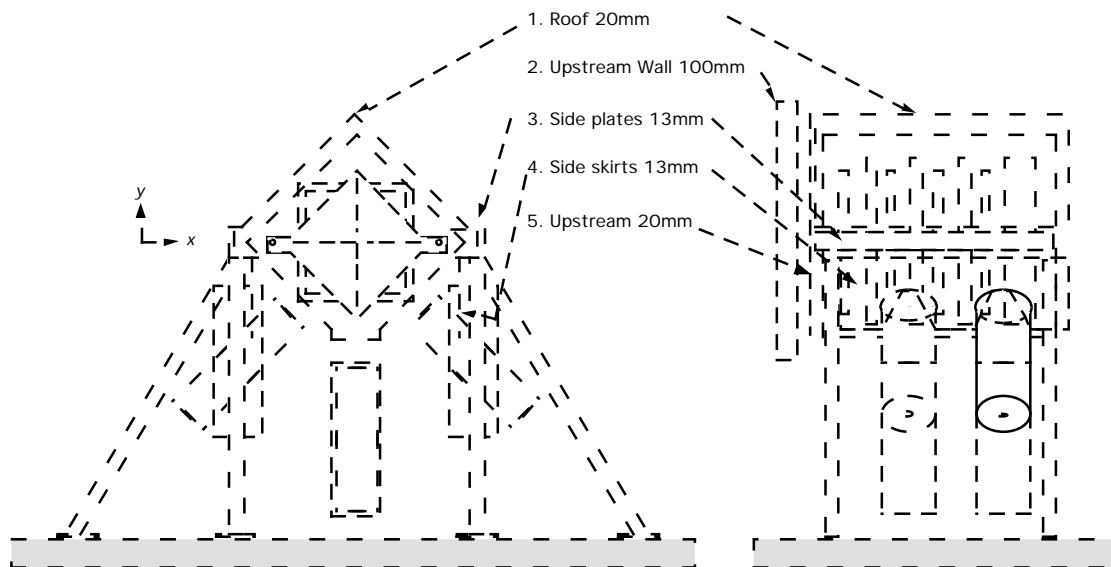


Figure 2. The E872 target box. The diagram depicts the support structure to elevate the target box into the prompt neutrino beam, lead shielding, target modules interspersed with

scintillating fiber detectors, and tubes containing the readout electronics for the scintillating fibers.

4.1 *Bulk Emulsion Modules*

type of emulsion detector, 95% of the module mass comprised of nuclear emulsion. Each sheet is made by coating both sides of a 100 μm plastic base with emulsion that dries to a thickness of 360 μm . These sheets, called bulk emulsion, are stacked together, using thin paper sheets as separators, to form a module. A bulk emulsion module contains 84 sheets for a mechanical structure 7 cm thick, of which 6 cm is emulsion. The production process for a bulk module requires 15 liters of emulsion gel.

4.2 *Emulsion Cloud Chamber Modules*

4.3 *Combination Modules*

4.4 *Changeable Sheets*

4.5 *X-ray sources*

To ensure that the proper region of the target is scanned, correct alignment of the changeable sheet with the target emulsion is crucial. This is accomplished with a set of ^{55}Fe radioactive sources, mounted in collimator on the supporting

structure for the target and the changeable sheets. Iron-55 decays via electron capture with a half-life of 2.73 years, producing an x-ray of approximately 6 keV. These x-rays make fiducial marks on the changeable sheets and on the target, allowing a precise alignment.

The sources were fabricated from plastic strips coated with ^{55}Fe on one side. The activity of the (new) sources was 120 - 150 kBq/mm². Disks 2 mm in diameter were punched from the strips and mounted in brass collimators with a screw which ensured that each source was the same distance from its collimator opening. This provided for uniformity in the fiducial marks. The collimator openings are 1 mm in diameter. Sixteen sources are arrayed on the front and back faces of each target module at intervals of 15 cm.

5 The Scintillating Fiber Tracker

A high resolution scintillating fiber detector is used in conjunction with the changeable emulsion sheets to predict the position of charged particle tracks in the emulsion. The track predictions must be made with sufficient precision to allow the automated scanning algorithms to find the tracks in the emulsion stacks. A system similar to that used for E872 was employed for this purpose in the CHORUS experiment at CERN [17]. The scintillating fiber detector consists of a series of planes of fibers interspersed with the target modules inside the target box, see Figure 3. The following sections describe the major elements of the scintillating fiber tracker.

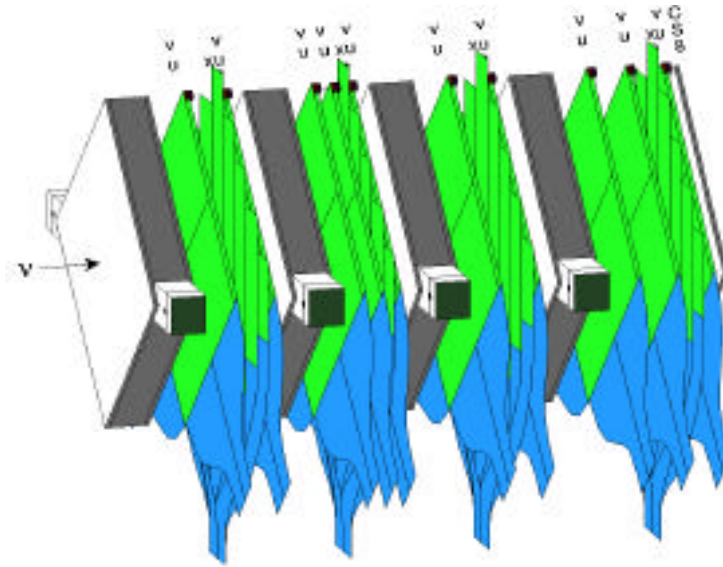


Figure 3: Emulsion target and scintillating fiber tracker configuration. The fiber planes are arranged in three views, the six image intensifiers and readout CCD cameras are not shown.

5.1 Scintillating Fiber Planes

There are 60000 scintillating fibers in the scintillating fiber tracker. Each fiber has a polystyrene center (core) doped with 1% butyl-PBD¹ and 0.1% BDB². The outer layer (cladding) of the fiber is made of PMMA³, which has a smaller index of refraction to produce total internal reflection of the scintillation light.

Each fiber has a diameter of 0.5 mm. The fiber length varies between 0.7m and 1.2m. An aluminum mirror with 85% reflectivity is put on one end of the

¹butyl-2-phenyl-5(4-biphenyl)-1-3-5-oxadiazole

²4,4'-bis-(2,5-dimethylstyryl)-diphenyl

³polymethyl methacrylate

fiber to increase the light output at the other end. The pulseheight response variation is less than 15% along the 0.56m of fiber that is glued into the plane (Figure 4).

The fibers are arranged to read out coordinates in u , v , and x . The u - v axes are oriented at 45° to the x - y axes, where the y axis is vertical. The fibers are placed side-by-side in layers, with 1200 fibers per layer. Each layer is coated with highly reflective TiO_2 - based paint that also serves as glue. The u and v planes each have two layers of fibers; the x planes have four layers. The plane configurations are illustrated in Figure 4 and Figure 5. Since the u and v planes are identical in their construction they are called uv planes. There are 44 planes of fibers altogether: 4 x planes, 20 u planes, and 20 v planes. Five planes of scintillating fibers are mounted downstream of emulsion modules one and three, four planes are mounted downstream of modules two and four.

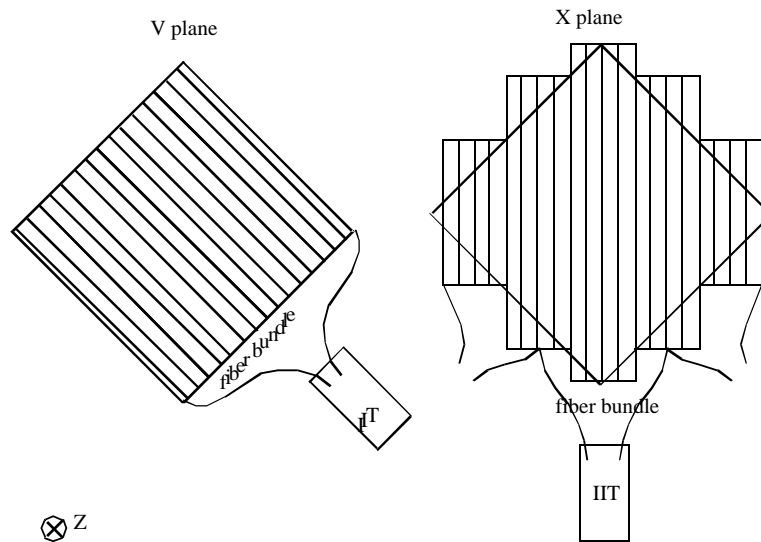


Figure 4. Front view of the fiber layout on a V and an X plane. Each plane has dimensions of 0.56m by 0.56m. Different sections of the X plane are connected to different IITs. The Z-axis points into the paper.

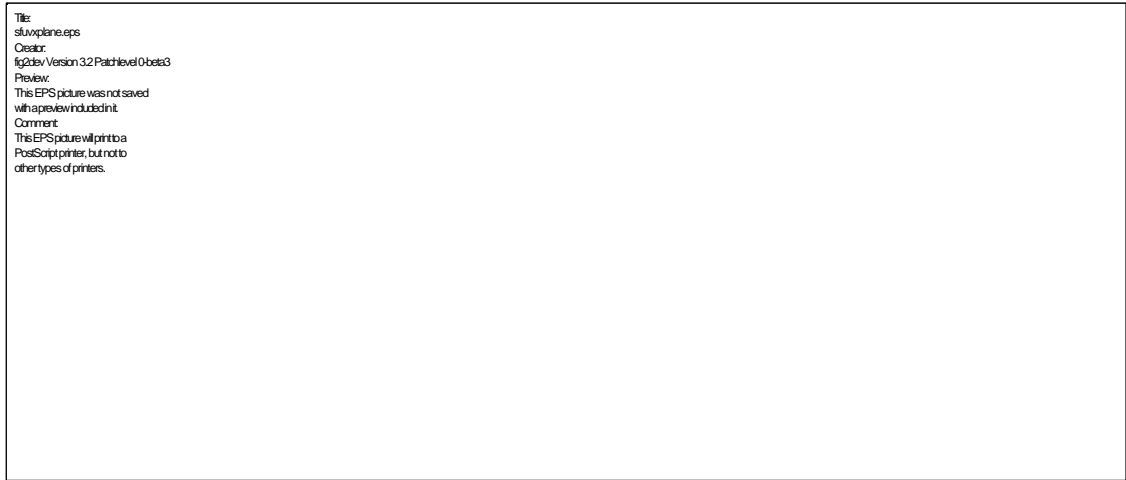


Figure 5: Fiber-on view of a scintillating fiber plane. The left-hand side shows the two layers of an UV plane, the right-hand side the four layers of an X plane.

Each plane has an area of 0.56m by 0.56m. In a uv plane, the fibers run parallel to a side; in an x plane they run diagonally, as shown in Figure 4. The average distance between a fiber plane and the readout system is 0.5m.

5.2 Image Intensifier (IIT) Modules

Six image intensifier (IIT) modules⁴ read out the fiber planes. Light from the fibers enters the IIT module and produces electrons in the photocathode of the

⁴ Image Intensifier type IC-5502X made by Hamamatsu Photonics, Japan.

entrance window, as shown in Figure 6. The electrons are focussed and accelerated in the first image intensifier stage.

At the output window of the first stage is a phosphor screen that converts the electrons into photons. The screen is connected to the photocathode of the next stage through a fiber-optic plate. This plate is made of millions of small diameter clear fibers that guide the light in a straight path. The fiber-optic plate is used to focus the light instead of a conventional lens system, which would take up much more space. There are four image intensifier stages. Each has a photocathode to produce electrons, electrostatic tubes to multiply the electrons, and a phosphor screen to convert the electrons into photons.

The IIT modules are shielded from the magnetic field of the analysis magnet with large soft iron canisters. The canisters reduce the fringe field, which reaches 150 G at the most upstream IIT, to an acceptable level below 0.2 G. The canisters are depicted in Figure 2.

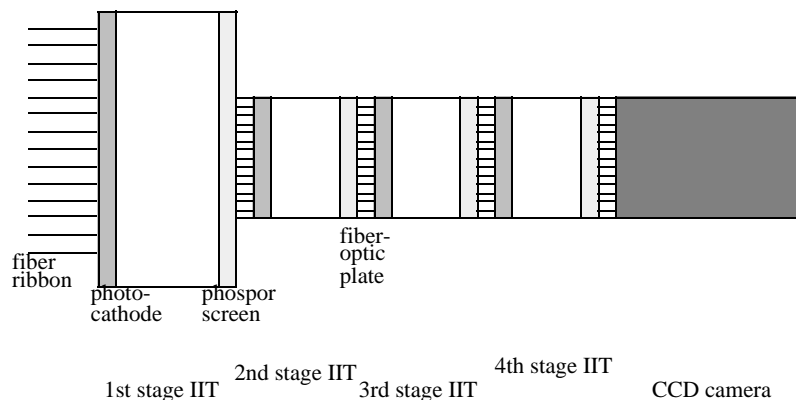


Figure 6: Layout of the IIT-CCD system.

The performance of the IIT module is determined by two parameters:

1. The quantum efficiency of the first stage. This is the probability that an electron will be emitted when a photon strikes the photocathode. When only a few photons reach the photocathode, this number determines the probability that a signal will be produced. The quantum efficiency is 20%.
2. The overall light multiplication factor or gain. This is the number of photons that exit the phosphor screen of the fourth stage when one photon strikes the photocathode of the first stage. This factor is $3-4 \times 10^6$ for the IIT modules.

The phosphor screen of the fourth IIT stage is mounted on a charged coupled device (CCD) video camera module through a fiber-optic plate. The camera has a sensitive area of 8.8mm by 6.6mm that is divided into 768 by 493 pixel⁵. About half of the CCD image area is occupied by fibers.

An eight-bit flash ADC that was custom-built for this experiment digitizes the pulseheight from the CCD camera. The pixels are read out at a rate of 14MHz.

The image intensifier stages map each scintillating fiber onto a circle with a diameter of about three pixels on the CCD camera, which corresponds to a demagnification factor of 0.034. The diameter is slightly larger (approximately 20%) at the edge of the image due to non-uniformity of the IIT. The CCD is read

⁵ CCD video camera XC-77RR made by Sony, Japan.

out into a VME-based FIFO memory buffer. The mean readout time for a single event is 24ms and this is the dominant factor in the deadtime for data acquisition.

5.3 Alignment

Aligning the scintillating fibers is a critical task in the experiment. To locate a vertex in the emulsion successfully, the vertex position has to be predicted with an accuracy of about 1mm^2 in the uv plane and about 10mm in Z .

To align the fibers with respect to the global E872 coordinate system, each SF plane is surveyed before it is mounted in the target stand. Fiber location, offset and angles between fibers are recorded in the survey. Also, the exact position of the stand itself is determined.

Once the plane is in place, cosmic ray muons and muons produced by proton beam losses upstream are used to align the fiber plane with respect to each other and with respect to the other detector components. Alignment of the fiber planes is periodically monitored with single muons that pass through the detector. A special trigger allows the muons to be added to the data stream. More detailed alignment information is also gathered in dedicated muon calibration runs.

The result of the fiber alignment is shown in the form of a histogram of residuals. A muon track that passes through all 44 SF planes is fitted with points from 43 planes and the projection to the remaining plane is calculated. The residual is defined as the distance between the track position and the hit that would have been used in the track. The histogram of residuals is shown in figure 5. The distribution has a standard deviation of about 0.17mm.

The maximum distance between fiber planes along the z axis behind a single emulsion module is 0.1m (except for module 4). That means the angle of a track can be determined to an accuracy of 3.3 mrad, as shown in Figure 8. As Figure 8 also shows, the track location projected to the changeable sheet can be determined to within a distance of about 0.35mm. Projected to the center of the emulsion module, this translates to within a distance of about 0.5mm.

The fibers also have to be aligned on the face of the CCD camera. Mapping the fibers to CCD coordinates cannot be done at assembly time because of the IIT system and the size of the fiber image. An optical calibration system monitors the location of a few fibers on the CCD image. In each SF plane, some of the fibers are connected to an electroluminescence (ELP) plate. Light from these “fiducial fibers” is easily found on the CCD image. The fiducial image is taken in between runs; the light is turned off during data acquisition. A map is created from the fiducial information that contains the location in space and on the CCD image for each fiber.

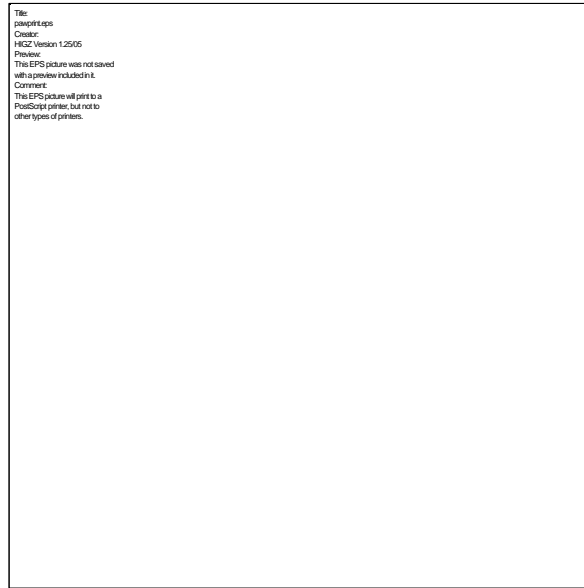


Figure 7: Histogram of the distance between track projection and hit position for SF hits in events from a muon run.

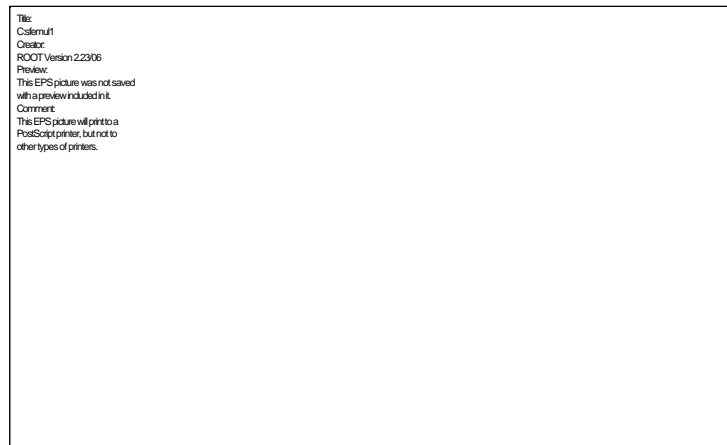


Figure 8: Histogram of the projection error from the SF system to changeable sheet CS5. The upper row shows the angle deviation for U and V planes, the lower row shows the position deviation for U and V planes. The solid line is a Gaussian fit to the histogram.

The location of each fiducial fiber can be determined to better than a fraction of a pixel. A typical fiber hit deposits a pulseheight in an area larger than 3x3 pixel. The location of each fiber on the CCD image is therefore very well known, but the pulseheight from a single fiber spreads to several fibers on the IIT image.

The fiber plane efficiency is measured to be 96% for a *uv* plane using cosmic rays. The efficiency for an *x* plane is estimated to be 99.8%.

6 The Trigger and Data Acquisition System

6.1 Trigger System

The goal of the trigger system is to select neutrino interactions with minimum bias and high efficiency while maintaining a small overall trigger rate to minimize readout dead-time. To maintain a live-time of > 85% required a trigger rate of 6 Hz or less during a spill. This condition is dictated by the scintillating fiber system CCD read-out time of 24 ms. The expected neutrino interaction rate at full beam intensity was tens of mHz.

6.2 Trigger Hardware

Trigger hodoscopes, designated T1, T2, T3, and V, were employed to select neutrino interactions and reject backgrounds from the intense flux of muons generated in the tungsten dump.

The most upstream component of the spectrometer is a veto wall consisting of 10 scintillation counters covering an area of 140 cm × 152 cm. The dimensions of each counter are 30.5 cm in *x*, 152 cm in *y*, and 10 cm in *z*. The counters are read out on each end by 5 inch EMI 9791 phototubes. This wall provides a charged particle veto signal for the neutrino interaction trigger. The veto wall is

arranged in two layers to maintain a high efficiency. The counters were measured to have better than 95% efficiency individually and veto wall efficiency was better than 99%.

A plane of scintillating fibers is located downstream of each of the fiber modules 2 and 4. These planes are designated T1 and T2, respectively. Each plane is 70 cm \times 70 cm in area and segmented into eight (T1) or nine (T2) 10 cm bundles. Each bundle is read out by a Hamamatsu R5600 phototube.

A scintillator hodoscope, T3, is located downstream of the target/fiber system. T3 is composed of 8 counters, each 10 cm \times 80 cm. The counters are 5 mm thick and are attached to 49 cm long light guides with phototubes (Philips 2262B 12 stage tubes) on each end. Each of the trigger counters had an efficiency of better than 97% for minimum-ionizing particles.

The main trigger required:

- hits in T1, T2, and T3 consistent with at least two charged tracks;
- track angles ($\tan \theta$) with respect to the neutrino beam axis of ≤ 250 mr ;
- no hits in V (veto wall).

Figure 9 shows the trigger logic for the E872 experiment.

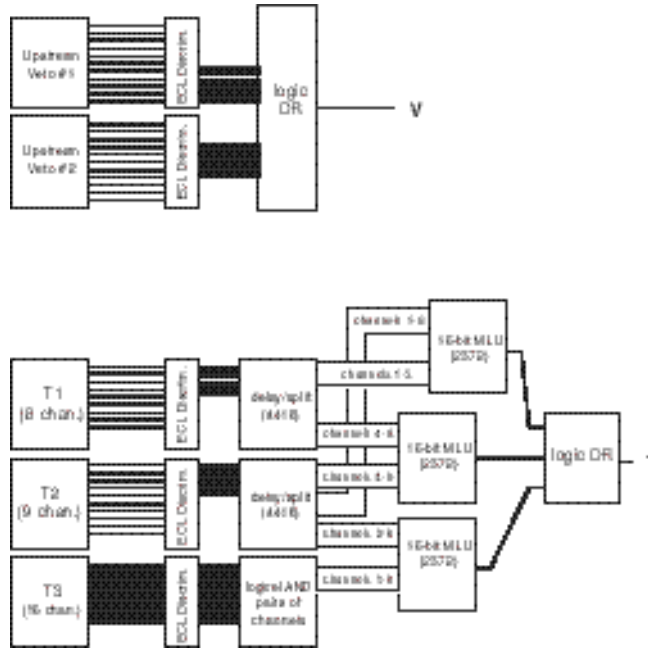


Figure 9 E872 trigger logic.

	T1	T2	T3	V
No. of counters per plane	8	9	8	5
No. of planes	1	1	1	2
Counter Width (cm)	10	10	10	30.5
Counter Length(cm)	20(2), 40(2), 60(2), 80(2)	10(2), 30(2), 50(2), 70(2), 80(1)	80	152.4
Counter Thickness (cm)	~0.3	~0.3	.4	10.2
Total Area (cm ²)			6400	20,917

Table 1. Parameters of the E872 trigger counters.

7 The Drift Chamber Tracking

Tracking and momentum measurement downstream of the emulsion target was accomplished with an air-core analysis magnet, ROSIE, and a set of drift chambers. A set of vertexing drift chambers (VDCs) was present inside the ROSIE aperture throughout the data run. A second set of large drift chambers (DCs) was present downstream of ROSIE throughout the run. Finally, a third set of drift chambers (KSX, KSY) was added inside the ROSIE aperture during the run.

7.1 ROSIE

7.2 Drift Chambers

Proceeding from downstream mirror plate of the ROSIE magnet the along the beam direction, drift (jet) chambers (VDC1, VDC2 and VDC3) near the upstream pole face. Immediately downstream of the ROSIE magnet are 3 prodigious drift chambers (DC1, DC2 and DC3) of conventional type.

The large downstream chambers are used with the analysis magnet for momentum measurement of charged particle tracks and to match upstream tracks to hits in the muon identification system and in the lead glass calorimeter.

7.2.1 The VDCs

The VDCs, or jet chambers, supplement the scintillating fiber system in track discrimination. The most downstream of the VDCs (VDC3) is located approximately 44 cm from the upstream face of the upstream mirror plate of ROSIE. The wires inside this VDC are slanted at a 4.2° angle from the vertical (u'), the middle VDC (VDC2) has wires slanted at -4.2° with respect to the

vertical (v'). The most upstream of the VDCs (VDC1) has wires oriented along the vertical direction (x plane). The active area of the VDCs is $100\text{ cm} \times 70\text{ cm}$. The chamber windows are centered 1.24 mm west of beam center.

Each VDC has 16 cells each 7 cm wide (perpendicular to beam) and 9 cm in depth. Each cell has 6 sense wires spaced in 0.95 cm increments along the z direction. The cell geometry is shown in Figure 10.

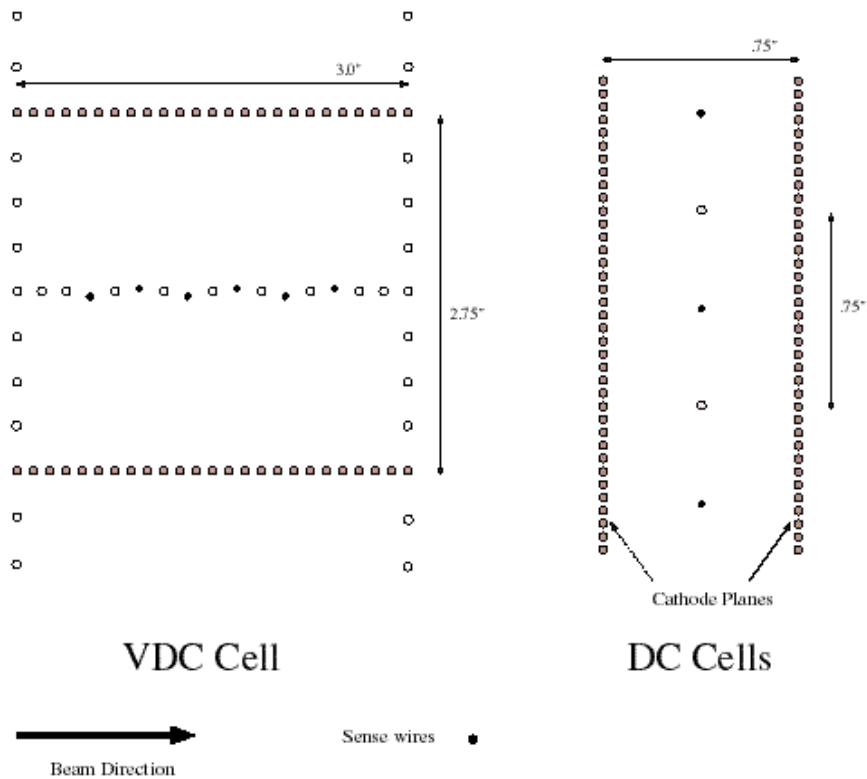


Figure 10. Cell geometry of the vertex (jet) drift chambers and of the large downstream drift chambers.

The cathode and field-shaping wires in the VDCs are $150\text{ }\mu\text{m}$ in diameter. The sense wires are and have a $25\text{-}\mu\text{m}$ diameter. The sense wires are staggered

on each side of the plane formed by the field wires. This staggering helps to resolve ambiguities in determining which side of the cell the particle actually traversed. The spacing between the field plane and one cathode plane is 3.5 cm. The guard wires are used to step the voltage down smoothly from the cathode to ground.

The VDCs have pre-amplifier cards on-board which output a differential analog signal. This feeds into a shaper/discriminator card whose purpose is to take groups of six signals (the number of pre-amp outputs) and regroup them in sets of eight signals so that no TDC channels will be wasted. The cards put out differential ECL signals that are routed to a crate of LeCroy 4291 TDCs. The TDCs are run in common stop mode so those hits closest to the wires will give the largest TDC values.

7.2.2 Supplemental VDCs

To improve tracking inside the magnet volume, two additional jet chambers were added during the summer of 1997. Each measured transverse position with four samples along the beam direction. Chamber KSY (17 cells) measured vertical (y) position, and was in place for about 2/3 of the data run. Chamber KSX (22 cells) measured horizontal (x) position, and was in place for about 1/3 of the data run. Both used LeCroy 2235 drift chamber amplifier-discriminators and multi-hit TDC's. These magnet chambers were designed to perform well in magnetic fields of tens of kilogauss, to minimally reduce the useful aperture of the magnet, and to work reliably in an inaccessible location. They used an 80%-20% ArCO₂ gas mixture, which has a small Lorentz angle but requires good drift field shaping because the drift velocity depends strongly on drift field.

Each cell had a drift distance of 3.3 cm. The four 25 μm sense wires, 1.016 cm apart, were staggered alternately by $\pm 254 \mu\text{m}$ in the drift direction to help resolve the left-right drift ambiguity. The sense wire plane contained an additional 9 “potential” wires of gold-plated aluminum 160 μm in diameter, located between the sense wires and extending the sense wire plane; these shaped the drift field. The chambers were typically operated with sense-wire voltage at 4,000 V and potential wire voltages chosen to give a uniform drift field of 660 V/cm. Some aspects of chamber performance are shown in Figure 11. On single muons, the chamber efficiency was better than 99% and the minimum-ionizing signals were exceptionally clean, with noise and afterpulsing less than 12%.

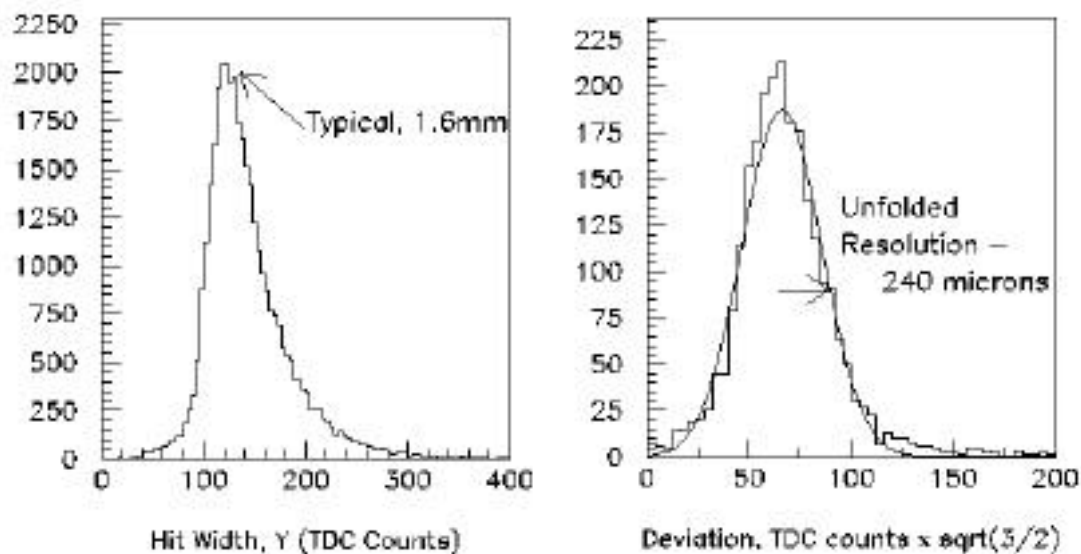


Figure 11. Performance of magnet chamber KSY on single muons. Left: Histogram of time-over threshold, showing a Landau distribution typically 1.6 mm wide in the drift direction. Right: unfolded resolution, before corrections for field-dependent drift velocity in ArCO_2 .

7.2.3 Physical Layout of the DCs

The three large DCs are situated between the ROSIE magnet and the lead glass house and we have labeled the most upstream of these DC1 (with DC3 being farthest downstream). Each of the DCs has chamber windows that are on both sides of aluminum frames. Each DC is approximately 30 cm deep. The first lies about 1 m downstream of the geometrical center of the analysis magnet. The second is positioned 75 cm downstream of the first and the third is 75 cm downstream of the second. The ordering of the planes in DC1 and DC2 from upstream to downstream is: ground plane, cathode plane, x' sense plane (with wires oriented vertically), cathode plane, x sense plane (with wires oriented vertically, but shifted by 9.5 mm from the previous vertical plane), cathode plane, u'' sense plane (with wires slanted from the vertical by 16.7 degrees with the top of the wires closest to the east wall), cathode plane, v'' sense plane (with wires slanted from the vertical by 16.7 degrees, with the top of the wires closest to the west wall), cathode plane and ground plan. Similarly, for chamber DC3 (previously used in Fermilab experiment E771 [18]) the ordering from upstream to downstream is: ground plane, cathode plane, x' sense plane, cathode plane, u'' sense plane, cathode plane, x sense plane, cathode plane, v'' sense plane, cathode plane, ground plane.

Each sense plane has alternate sense and field-shaping wires spaced 9.5 mm apart. Each cathode plane has cathode wires spaced 2.1 mm apart.

Alternating cathode/sense/cathode planes every 9.5 mm along the beam direction create drift cells. The cell geometry of the DCs can be seen in Figure 10.

Each of the DCs was constructed to have 176 cells of one sense wire each. For DC1 only the center 112 cells of the x and x' planes and the center 144 cells of the u'' and v'' planes are used. This is an active width of 223 cm. For DC2 and DC3 all 176 cell of the x and x' cells are used. The center 176 cells are used for the u'' and v'' planes of DC2 and the u'' plane of DC3. The v'' plane of DC3 uses only its central 144 cells.

The drift chambers use a gas mixture of 50% Ar and 50% ethane. A customized system in the gas shed precisely controls the mixture of the two gases. The gas is routed to the chambers through a system of bundle tubing, with the option of bubbling the gas through ethanol at 0°C for suppression of corona discharges. A solenoid at the gas inlet to the chamber and a second solenoid at the outlet regulate each chamber's pressure.

DC1 and DC2 were constructed as identical chambers and employ exactly the same signal amplification electronics. The geometry of DC3 is the same as for DC1 and DC2, but its field wires have a larger diameter and its amplifier cards are entirely different. All three DCs output differential ECL signals (via their amplifier cards) to LeCroy 4291 TDC modules.

7.2.4 Drift Chamber Resolution

Resolution for both the VDCs and the DCs were measured with muons from the PW5 dump. Single, unambiguous muon tracks (as identified in the muon identification system) were fitted and the residual distance to the hit

position on the sense wires was calculated. Histograms of the residuals for the VDCs and DCs are shown in Figure 12 and Figure 13, respectively.

7.2.5 Drift Chamber Efficiencies

The efficiencies of the drift chambers were found by using muons from the PW5 dump. The efficiency is taken to be the fraction of the time that a sense wire did not give a signal for a clearly defined muon track, subtracted from unity. For the VDCs the combined efficiency of the all the 1st, 2nd, etc. sense wires in all the cells is shown in Figure 14. The efficiencies for entire planes of sense wires in the DCs are shown in Figure 14 as well.

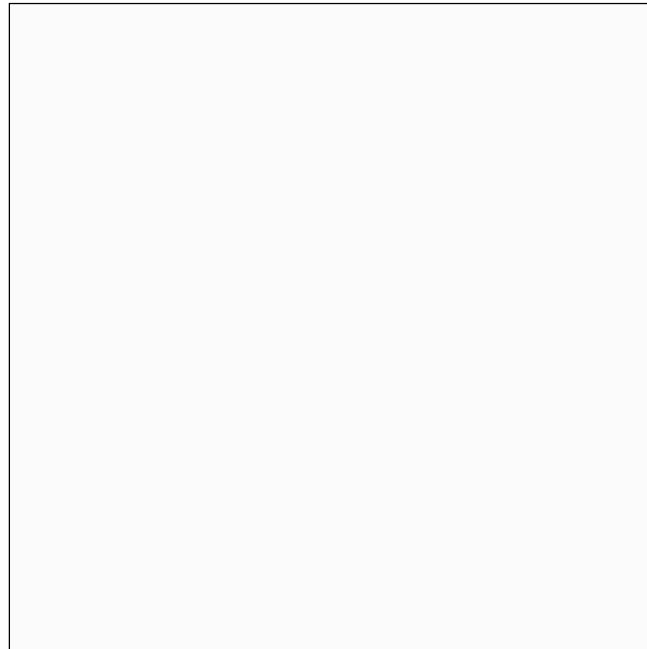


Figure 12. Gaussian fits to residuals (difference of track and hit positions) used to determine the resolution of the VDCs.

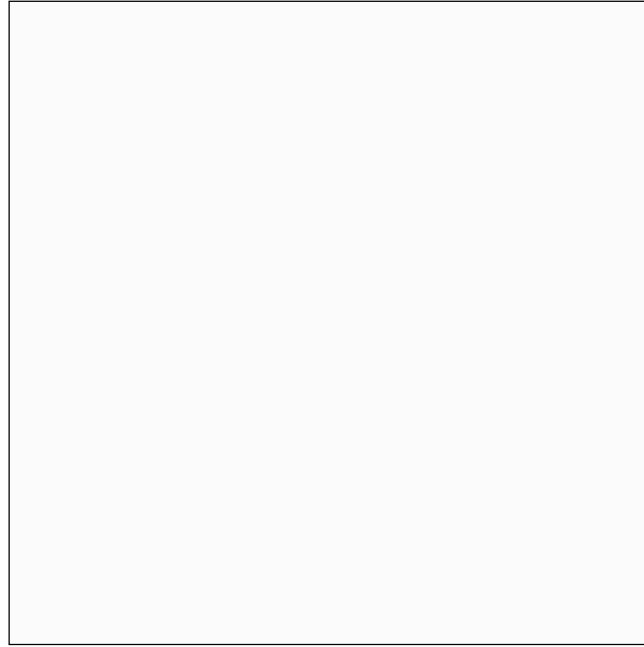


Figure 13. Gaussian fits to residuals (difference of track and hit positions) used to determine the resolution of the large DCs.

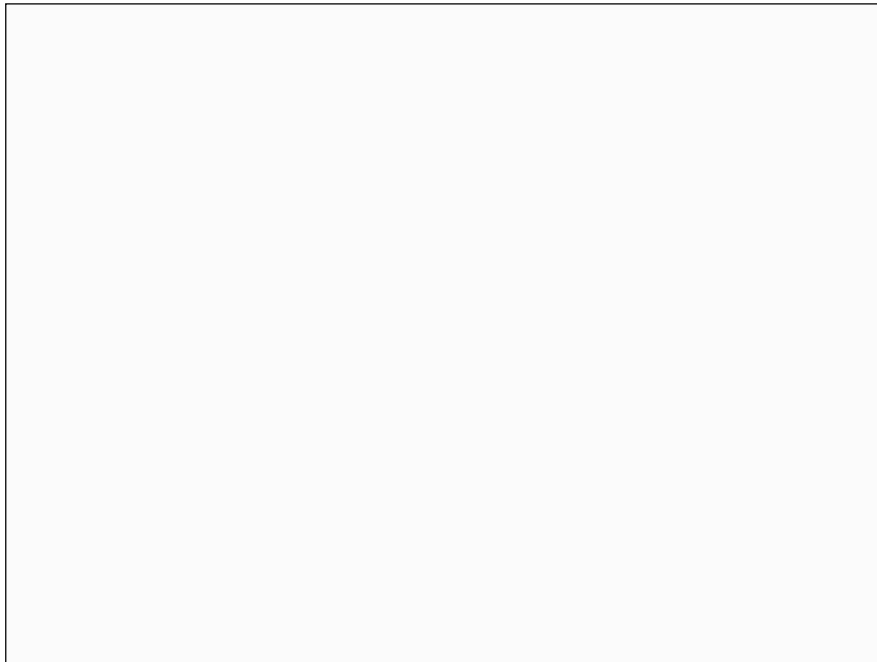


Figure 14. Drift chamber efficiencies for the VDCs (top) and large drift chambers (bottom).

8 Electromagnetic Calorimeter

The purpose of the electromagnetic calorimeter (EMCAL) is to aid in the identification of electromagnetic energy coming from e^+e^- interactions or from electrons produced in μ decays. The energy measured in the calorimeter is also used in determining the total energy of a neutrino interaction.

The EMCAL is a wall comprising 400 elements of lead glass and scintillating glass instrumented with photomultiplier tubes. Its dimensions, as seen from the beam view, are 375 cm \times 195 cm. The central region is made of SCG-1 scintillating glass blocks, while the outer regions are made of SF5 lead glass blocks. The parameters of the blocks are given in Table 2.

Glass	# Blocks	Dimensions (cm)	Location	Depth (em)	Depth (nucl)	Phototube
SCG1-C	100	7.5 \times 7.5 \times 89	Center	20.9	2.0	RCA 6342A
SCG1-C	74	15 \times 15 \times 89	Intermediate	20.9	2.0	EMI 9791KB
SF5	224	15 \times 15 \times 41.5	Outer	16.8	1.0	EMI 9791KB

Table 2 Parameters of the glass blocks used in construction of the EMCAL. The columns Depth columns list the depth of the blocks along the beam direction in radiation lengths (em) and nuclear absorption lengths (nucl).

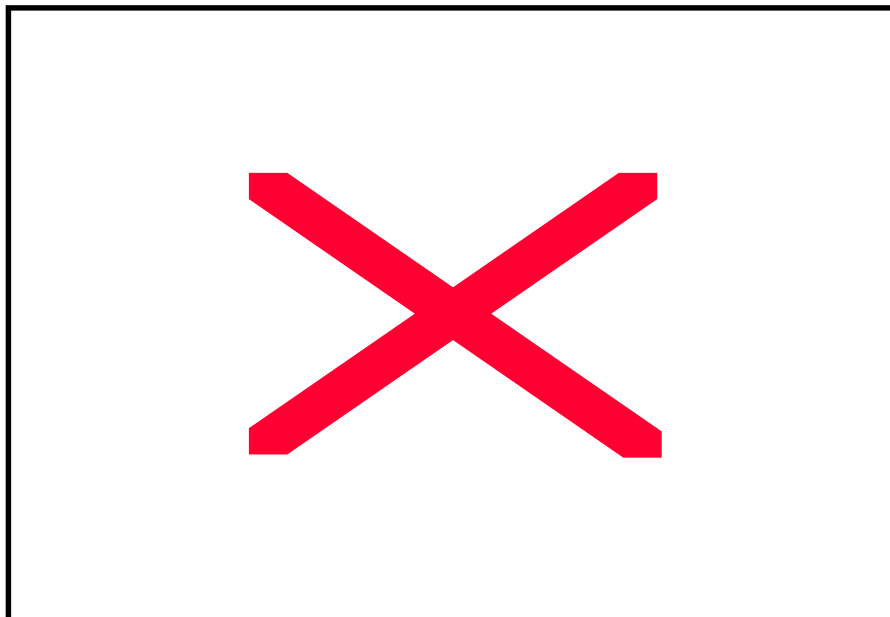
The smallest blocks, which are of scintillating glass, are placed in the central region of the wall. They are surrounded by larger scintillating glass blocks and finally by lead glass.

A schematic diagram of the EMCAL system is shown in Figure 15. A pair of LeCroy 1440 high voltage power supplies provided power for the photomultiplier tubes. The voltage on each tube was adjustable through a

Pentium PC computer connected to the system through a serial RS-232 line. The anode signals from the PMTs were connected via RG8U cables to a passive splitter, where a fraction of each signal was used as an input to a calorimeter trigger system. Most of the signal (80%) was delayed by 450 ns and read by LeCroy 2280 ADCs. The RG8U served to minimize signal loss, dispersion and noise due to the long cable runs. The integrating gate widths were 260 ns for the lead glass blocks and 350 ns for the scintillating glass blocks, the difference being due to the longer decay time of the latter.

An LED system continuously monitored the performance of the EMCAL to track and correct for gain variations of the PMTs. Optical fibers of 0.3 mm diameter distributed the LED light to the surface of the blocks. The LED measurements and the pedestals were read out between spills of the proton beam. The LED system, combined with muon measurements taken during the experiment, was crucial in the calibration of the EMCAL. Studies found the

stabi
was :



system

Figure 15. A schematic overview of the electromagnetic calorimeter system.

A representative sample of blocks, including all three types, was tested in a beam at Brookhaven National Laboratory before the experimental run at Fermilab. The blocks were exposed to electrons, pions and muons. The EMCAL calibration used the electron/muon response measured in the test beam. The energy resolution of the individual blocks at 1 GeV was about 6.5% for the lead glass, 7.5% for the large scintillating glass, and 12.5% for the small scintillating glass. Due to the lack of a calibration beam during the run, we expect a somewhat poorer overall energy resolution, but not worse than 20% at 1 GeV. Typical muon and electron energy distributions are shown in Figure 16 a and b.

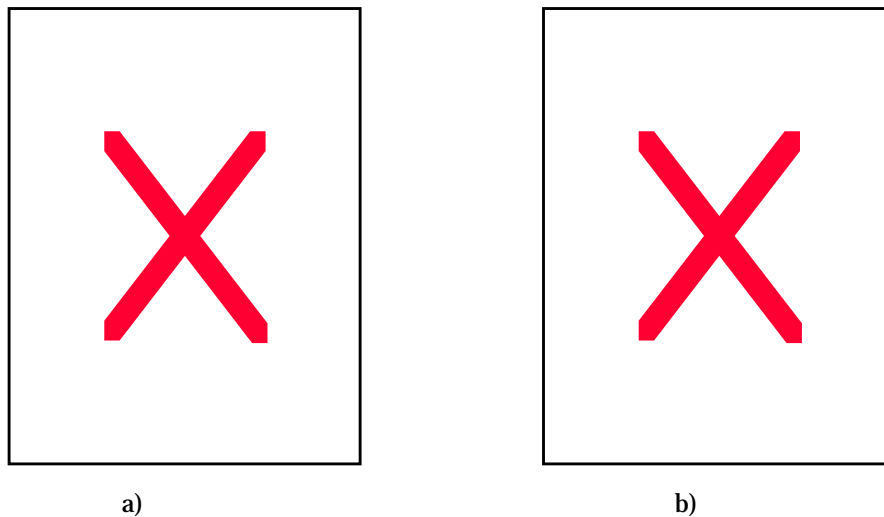


Figure 16. ADC response of a xxx block to minimum-ionizing particles a) and 2 GeV electrons b) in the Brookhaven test beam.

9 The Muon Identification System

The primary purpose of the muon identification system (MUID) is to identify muons coming from the charged-current interaction of muon neutrinos in the emulsion target. In such interactions the muon track will point back to the primary interaction vertex and hence can be rejected as a candidate for a interaction. The MUID system will also identify muons from muonic decay of a lepton. Tau leptons decay via the muon channel 17% of the time.

The muon identifier is a three-layer array of steel walls and planes of particle detectors. The upstream steel wall is 3.7 m high by 6.25 m wide and is 0.42 m thick. The two remaining walls are each 3.25 m high by 5.48 m wide and 0.91 m thick. There are air gaps of 80 – 82 cm between the walls. The total system is 4 m in length. Planes of detectors are placed between the walls to measure the vertical and horizontal positions of charged particles emerging from the steel. Proportional tubes cover 80% of the cross section; the remainder is covered by scintillator hodoscopes. The detectors were constructed at Tufts University and shipped to Fermilab in the summer and fall of 1996.

9.1 Proportional Tubes

There are three stations in the MUID system, referred to as A, B, and C, with A the farthest upstream. Each station consists of two H-shaped planes of proportional tubes, one each for x and y readout. The gaps in the H are where the muon flux was most intense.

The principal structural element of the proportional tubes is a four-cell aluminum extrusion. Each cell is a square 4 cm on a side. A total of 248 four-cell

modules were constructed with lengths ranging from 1.3 to 6.25 m to accommodate the H-shape of the planes. The A planes are somewhat larger than those at stations B and C to improve the acceptance for low-momentum muons coming from the emulsion target. The proportional tubes are operated with a 95% - 5% ArCO₂ gas mixture. Each cell contains a 60- μ m sense wire. The current signals from the sense wires are processed by a four-channel amplifier/discriminator card mounted on each module. The discriminator outputs are translated on the card to differential ECL levels for transmission over 100 m of twisted pair cable to coincidence registers.

9.2 *Scintillator Hodoscopes*

Scintillator hodoscopes fill apertures in the proportional tube planes left in the regions on both sides of the beam line where there is an intense flux of muons from the dump. The 1- μ sec resolving time of the proportional tubes is too long to handle this intense flux. The resolving time of the scintillator elements is approximately 15 ns. There are six scintillator hodoscopes, one each at the east end and the west end of the three MUID stations. Each hodoscope has an x and y readout.

The width of the scintillator elements is 4 cm to match the proportional tube cell width. Each element is 1.5 cm thick. The range of element lengths is 1.0 m to 2.3 m. There are a total of 448 elements distributed over the six hodoscopes. The hodoscopes are constructed within aluminum boxes mounted on movable frames so as to position them in the gaps in the proportional tube stations. Each scintillator element is wrapped in aluminum foil for optical isolation. As this foil is at the same high voltage as the photocathode of the PMT, mylar sheets are

used to insulate the horizontal and vertical elements from each other and from the aluminum box. The interiors of the aluminum boxes were cooled by forced air.

Hamamatsu R1666 tubes epoxied to the scintillator are used to view 256 of the elements. The remaining 192 elements are viewed by a set of 12 Hamamatsu 16-ch multianode photomultiplier tubes. Waveshifting fibers of 4 mm square cross section are placed in grooves milled along the lengths of these 192 elements. The fibers are gathered in 4 by 4 bundles and coupled to the multichannel tube by optical grease. The distribution of detector elements at stations A, B, and C is detailed in Table 3.

Readout signals leave the hodoscope box via ribbon twist-n-flat cable, bypassing the preamp on the R1666 cards. The signals then go into 28 N277 Nanocards, which provide ECL output. Thus, the data acquisition system can handle all signals from the MUID system in the same way.

Station	Plane	Gas Tubes	Scintillators	Detector Elements
A	x	264	112	376
A	y	88	48	136
B	x	232	96	328
B	y	88	48	136
C	x	232	96	328
C	y	88	48	136
Total		992	448	1440

Table 3. Detector elements in the muon ID system.

9.3 *Muon ID Performance*

Measurements in a cosmic ray test stand at Tufts showed that the efficiency of the proportional tubes is 97%. The slight inefficiency can be attributed to the insensitive area between the cells formed by the 2 mm thick interior walls.

Muons from PW5 were used to align the proportional tube stations. Figure 17 shows plots of the residuals of hits extrapolated from drift chamber tracks and the actual prop tube hit. The fits to the data are Gaussian. The flattening of the peaks in the downstream walls is due to multiple scattering in the steel [19].

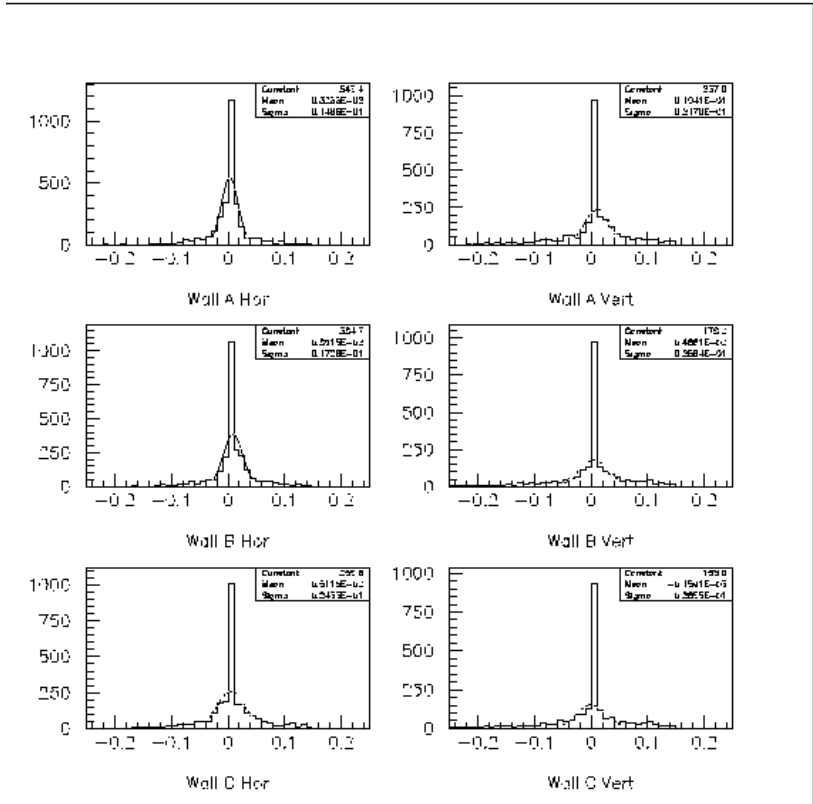


Figure 17. Alignment of the proportional tube stations of the muon ID system. Actual hits are compared with extrapolations from tracks using drift chamber information and the residuals plotted in 2 cm bins. Fits are Gaussian.

10 Emulsion Processing

The use of nuclear emulsions requires some special purpose facilities at the experiment and at the universities. For E872 the facilities are located at Japanese universities and at Fermilab. The pouring of all full-sized emulsion sheets is done at Kobe University. The sheets are shipped to Fermilab and stored prior to

use in a lead-shielded enclosure. The individual sheets are assembled into modules at Fermilab just prior to installation. The modules are built in aluminum fixtures that allow them to be mounted on the precision stand in the beamline. After exposure, the modules must be disassembled, the sheets removed, and marked with a grid pattern of 50 μ m dots that can be measured at scanning time. These dots, called a "grid print", give an accurate measure of the amount of shrinkage and distortion of the emulsion after it has been developed. This grid printing must take place in a carefully controlled environment which is dark, temperature held to $\pm 1^\circ\text{C}$ and humidity kept to $\pm 10\%$ of the relative humidity at which it was packed. This was done for the first run in a small extension to the target house surrounding the emulsion area in the beamline.

Development of all bulk type sheets is done in Japan at Nagoya University. All "thin" emulsion sheets, ECC type, are processed at Fermilab in darkroom / drying rooms at the New Muon Lab (NMS).

11 Emulsion Scanning

The use of automated scanning stations, pioneered at Nagoya University, has brought emulsion analysis into the digital era. The data recorded in the emulsion is extracted and summarized on standard mass storage media with speeds and efficiency that exceed human scanners by three orders of magnitude.

12 Data Analysis

The "standard" technique is to locate a well-reconstructed track from the electronic tracking detector into the emulsion stack, and follow this track until it ends at the interaction vertex. This method, also used in the CHORUS experiment, is appropriate for only about 50% of the data in DONUT. Because

the emulsion targets are very thick, 6cm, this method of following tracks from the spectrometer is less reliable for vertices in the upstream part of the target because of secondary interactions, electron showers, and scattering. A second method is used for upstream or complex events where the position of the vertex is poorly known. In this method, automatic emulsion scanning stations are programmed to find all tracks in a *volume* of emulsion surrounding the interaction prediction. This data is then processed by finding all 3-track vertices in this volume. For each DONUT event processed in this way, there are up to 10^4 tracks found in every 5 cm^3 of target emulsion. Almost all of these tracks are from background particles, and will not produce the proper topology of a neutral vertex. This powerful method is possible only because of the speed of the present scanning stations. Nevertheless, until March 1999, it required more than 10 hours to process one event in this way. Today at Nagoya University the next generation scanning machines are now on-line, and have proven speed increases of 8 to 10 over the previous generation.

13 Status

The experiment completed taking data in September 1997. A total of 4.5×10^{17} protons of 800 GeV energy were interacted in a beam dump to produce the tau neutrinos. An estimated 69 ± 24 interactions are recorded in the emulsion stacks.

In the past year, the analysis of the data has shifted from electronic reconstruction of the spectrometer data to the extraction of the emulsion data for the interactions identified by the detectors in spectrometer. Much effort has been spent in developing emulsion scanning techniques necessary for insuring high efficiency in locating the interactions in the emulsion.

The electronic reconstruction and the selection of neutrino interaction candidates are complete. The decay search for the characteristic kink signature is presently underway using the digitized emulsion data, in much the same way as the analysis of electronic detectors. Most of the neutrino interactions are e or μ , but we expect about 5% to be τ if the located sample is unbiased.

As of 15 Nov 1999, 203 events have been unambiguously located in the emulsion data out of 414 interaction candidates, selected out of 901 events. In addition, 105 events have been scanned but not yet processed for location, and approximately 110 more events are waiting to be scanned (followed by attempted location). The location efficiency, is now 60%, and therefore we expect about 130 more events to be located from this sample that is tagged for analysis. An additional 200 events could be located later, but have been excluded from the present sample for various reasons (e.g. high background, emulsion damage, low primary multiplicity, etc.). This work was supported by the U. S. Department of Energy under contract number DE-AC02-76CH03000.

References

- [1] B. Lundberg, *et al.*, Fermilab Proposal P872, 1994.
- [2] G. Kane, *Modern Elementary Particle Physics*, Addison-Wesley Publishing (1993) 270.
- [3] N. Ushida *et al.*, *Phys. Rev. Lett.* 57 (1986) 2897.
- [4] D. Buskulic *et al.*, the ALEPH Collaboration, *Z. Phys. C70* (1996) 561.
- [5] D. Abbaneo *et al.*, the LEP Electroweak Working Group, CERN-EP-015-99 (1999).
- [6] N. Ushida *et al.*, *Nucl. Inst. and Meth.* 224 (1984) 50.
- [7] K. Kodama *et al.*, *Nucl. Inst. and Meth. A* 289 (1990) 146.
- [8] E. Eskut *et al.*, the CHORUS Collaboration, *Nucl. Instr. and Meth. A* 401 (1997) 7.
- [9] Y. Fukuda *et al.*, Super-Kamiokande Collaboration, *Phys. Rev. Lett.* 81 (1998) 1562.

[10] A. Asratyan et al., ITEP Group of the E803/COSMOS Collaboration, ITEP-30-98 (1998).

[11] A. S. Ayan et al., the TOSCA Collaboration, CERN-SPSC/97-5 (1997).

[12] H. Shibuya et al., the OPERA Collaboration, LNGS-LOI 8/97 (1997)

13 Ibid.

14 Reference to the cross sections for each of the nt's.

15 N. V. Mokhov and J. D. Cossairt, Proceedings of the Fourth Workshop on Simulating Accelerator Radiation Environments (SARE4), Knoxville, Tennessee, 1998.

16 R. Schwienhorst, Ph.D. Thesis, University of Minnesota, 2000.

17 E. Eskut et al., Nucl. Inst. and Meth. A 401 (1997) 7.

18 T. Alexopoulos, et al., E771 Collaboration, Nucl. Inst. and Meth. A 376 (1996) 375.

19 M. Skender, Master's thesis, Tufts University, 1997.